

# Facile synthesis of nickel oxide nanotubes and their antibacterial, electrochemical and magnetic properties†

Huan Pang,<sup>a</sup> Qingyi Lu,<sup>\*a</sup> Yecheng Li<sup>a</sup> and Feng Gao<sup>\*b</sup>

Received (in Cambridge, UK) 22nd July 2009, Accepted 14th October 2009

First published as an Advance Article on the web 6th November 2009

DOI: 10.1039/b914898a

Nickel oxide nanotubes with great antibacterial activities, electrochemical capacitance, and magnetic properties have been synthesized through a precursor method with dimethylglyoxime as precipitant for the precursor, and the method has been developed for the synthesis of Ni/C nanorods.

Due to low mass density, high porosity, and increased surface area, hollow inorganic nanomaterials constitute an important family of nanostructures with interesting properties and potential applications, such as catalysts, host materials, sensors, drug-delivery carriers, acoustic insulation, biomedical diagnosis agents, and chemical reactors.<sup>1–4</sup> Up to now, some synthetic strategies have been developed to fabricate hollow inorganic nanostructures, such as the Kirkendall effect,<sup>5</sup> self-curling mechanism,<sup>6,7</sup> template-directed synthesis,<sup>8,9</sup> etc. However, these methods need complicated multi-steps such as removal of the template or selective etching in an appropriate solvent, which would make the product impure and limit the extensive applications of the nanotubes.

Nickel oxide (NiO) has been under extensive investigations as an important functional inorganic material and has diverse technological applications in fuel cell electrodes, heterogeneous catalysis, antiferromagnetic layers, etc.<sup>10–13</sup> The valuable functions greatly depend on the composition and structure. Of the wide range of nanostructures, nanotubes represent a perfect one-dimensional topology that hold the foreground as functionalized materials as a result of both shape-specific and quantum size effects. However, to the best of our knowledge there are few reports about the production of NiO nanotubes.<sup>14,15</sup> In the study presented here, we developed a simple and convenient approach for the synthesis of NiO nanotubes through one-dimensional metal complex bis(dimethylglyoximate) nickel(II), Ni(dmgl)<sub>2</sub>. The obtained NiO nanotubes show good antibacterial properties compared to commercial NiO and synthetic NiO nanoflowers. Also, the NiO nanotubes exhibit effective electrochemical capacitance, which can be used as a supply of energy in the exothermic system. The magnetic measurement demonstrates that unlike antimagnetic bulk NiO,<sup>16</sup> the NiO nanotubes are

magnetic and may be used in fields of MR imaging and magnetic drug delivery.

Dimethylglyoxime CH<sub>3</sub>(C=NOH)<sub>2</sub>CH<sub>3</sub> is a common organic precipitant for Ni<sup>2+</sup> in industry.<sup>17</sup> Herein, the precursor was easily synthesized by mixing dimethylglyoxime and Ni(OAc)<sub>2</sub> in aqueous solution with vigorous stirring (see ESI† for experimental details). X-ray diffraction (XRD) analysis and scanning electron microscopy (SEM) observation confirm that the obtained product is Ni(dmgl)<sub>2</sub> and has a one-dimensional morphology, with an average diameter of 600 nm (XRD pattern and SEM images are shown in Fig. 1a and ESI† Fig. S11, respectively). Dimethylglyoxime would chelate with Ni<sup>2+</sup> ion to form a square planar configuration with Ni<sup>2+</sup> in the center. The central metal Ni<sup>2+</sup> ions interact strongly with the adjacent molecules and the square planes stack face-to-face, resulting in a one-dimensional columnar structure as shown in Fig. S12.†<sup>18</sup> This inherent columnar structure would lead to the formation of Ni(dmgl)<sub>2</sub> nanorods.

After the precursor was calcined at 450 °C in air, NiO nanotubes can be obtained. The XRD analysis (Fig. 1b) confirms that the Ni(dmgl)<sub>2</sub> nanorod precursor has been completely transformed to NiO (JCPDS-780643). The XRD peaks are very broad, indicating that the NiO nanocrystallites are in the range of the nanometre scale. The rod-like morphology is maintained on a large scale, as evidenced by SEM image in Fig. 2a. But unlike the precursor, these 1D crystals are tubes, which can be clearly seen from Fig. 2b as there are holes of the broken ends. Fig. 2c displays an SEM image with a higher magnification, confirming that the product is one-dimensional nanotubes, and the surface is very rough, suggesting that the nanotubes might be composed of NiO nanoparticles. The

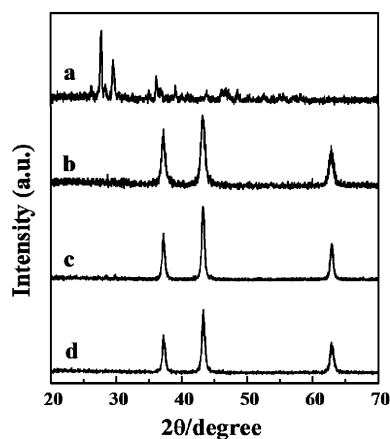


Fig. 1 XRD patterns of (a) Ni(dmgl)<sub>2</sub> nanorods; (b) NiO nanotubes; (c) commercial NiO; (d) NiO nanoflowers.

<sup>a</sup> State Key Laboratory of Coordination Chemistry, Coordination Chemistry Institute, Nanjing National Laboratory of Microstructures, Nanjing University, Nanjing, 210093, P. R. China. E-mail: qylu@nju.edu.cn

<sup>b</sup> Department of Materials Science and Engineering, Nanjing University, Nanjing, 210093, P. R. China. E-mail: fgao@nju.edu.cn

† Electronic supplementary information (ESI) available: Experimental details; SEM images, molecular structure, and TG curve of Ni(dmgl)<sub>2</sub> nanorods; SEM images of NiO nanoflowers and commercial NiO; variation of specific capacitance with cycle number; XRD pattern, SEM and TEM images of Ni/C nanocomposite. See DOI: 10.1039/b914898a

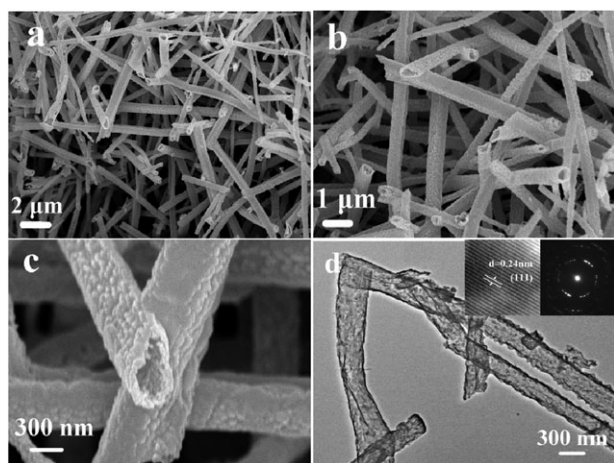
diameter of an individual nanotubes is about 300 nm, much smaller than the diameter of the original Ni(dmg)<sub>2</sub> nanorods. This is reasonable because during the thermal decomposition the remarkable shrinkage would occur as gases (such as CO, CO<sub>2</sub>, and H<sub>2</sub>O) are generated, and the weight loss is as high as about 75%, as the TG curve of Ni(dmg)<sub>2</sub> shows (Fig. S13).<sup>†</sup> The transmission electron microscopy (TEM) image shown in Fig. 2d also demonstrates that the product has tube-like nanostructures with an average inner diameter of 200 nm and the NiO nanotubes are composed of nanoparticles, which leads to the polycrystalline SAED pattern (Fig. 2d right-inset). A high-resolution HRTEM image (Fig. 2d left-inset) displays clear lattices of NiO crystal, confirming the crystalline nature of NiO nanotubes. During the process with Ni(dmg)<sub>2</sub> nanorods acting as a self-sacrificial template for NiO nanotubes, the transformation from Ni(dmg)<sub>2</sub> to NiO would start at the surface of the solid nanorods. Subsequently, NiO nanocrystals crystallize and form a polycrystalline layer on the surface of the nanorods. In the following growth process, Ni(dmg)<sub>2</sub> precursors continue to be consumed and the transformation continues toward the interior of the nanorods. Thus, the smooth solid nanorods gradually convert into rough porous nanorods and finally to completely porous hollow nanotubes because of the large mass lost during the transformation.

NiO nanomaterials have wide applications in many fields, however little literature has reported the antimicrobial activities of NiO. In this study, we studied the antimicrobial activities of NiO nanotubes against *B. subtilis*, *S. aureus*, *S. faecalis*, *P. aeruginosa*, and *E. cloacae* by determining the minimum inhibitory concentrations (MIC,  $\mu\text{g mL}^{-1}$ ) through a colorimetric method using the dye MTT (3-(4,5-dimethylthiazol-2-yl)-2,5-diphenyltetrazolium bromide).<sup>19,20</sup> For comparison, the antimicrobial activities of commercial NiO and synthetic NiO nanoflowers (the synthesis details are described in the ESI<sup>†</sup> and the XRD patterns and morphologies of commercial NiO and NiO nanoflowers are displayed in Fig. 1 and Fig. S14<sup>†</sup>) have also been investigated. The results are presented in Table 1 and demonstrate that the NiO nanotubes can kill all of the tested five bacteria well, especially

*B. subtilis*, *S. aureus* and *P. aeruginosa*, while the commercial NiO and the NiO nanoflowers have no or very weak antibacterial abilities to the tested five bacteria. Although the real mechanism of the antibacterial effect is still uncertain, there is no doubt that this effective antibacterial ability of NiO nanotubes would arise from its special nanoparticle-composed tube-structure, in which its hollow interior might inhibit the growth of bacterial and the high specific surface area would increase the efficiency of antimicrobial performance (the BET surface areas are  $2.9 \text{ m}^2 \text{ g}^{-1}$ ,  $10.3 \text{ m}^2 \text{ g}^{-1}$ ,  $27.0 \text{ m}^2 \text{ g}^{-1}$  for commercial NiO, NiO nanoflowers, and NiO nanotubes, respectively).<sup>21</sup>

The electrochemical properties of NiO nanotubes were investigated by cyclic voltammetry (CV), and chronopotentiometry (CP). Fig. 3a shows CV curves, with different scanning rates, of the NiO nanotubes. The shapes are different from that of electric double layer capacitance, which normally shows an approximately rectangular shape. Typically, a couple of redox peaks can be observed within the potential range 0.3–0.5 V, and the peak currents are linearly proportional to the sweep rate, suggesting that the capacity mainly results from pseudocapacitive capacitance, which is based on a redox mechanism. Fig. 3b shows the typical chronopotentiograms of the NiO nanotubes electrode measured in the potential range of 0–0.5 V. It obviously displays two variation ranges during the discharge steps: a linear variation of the time dependence of the potential (below about 0.30 V) indicating the double-layer capacitance behavior, which is caused by the charge separation taking place between the electrode and the electrolyte interface, and a slope variation of the time dependence of the potential (from 0.50 V to 0.30 V), indicating a typical pseudocapacitance behavior, which results from the electrochemical redox reaction at an interface between electrode and electrolyte.<sup>22</sup> The specific capacitance of the NiO nanotube electrode can be calculated to be 80.49, 73.39 and  $46.74 \text{ F g}^{-1}$  when the current densities are 50, 80, and  $280 \text{ mA g}^{-1}$ , respectively. On the other hand, as a long cycle life is very important for electrochemical capacitors, the cycle charge/discharge test has also been employed to examine the service life of the NiO nanotubes. Fig. S15<sup>†</sup> shows the variation of specific capacitance with cycle number at 4.5 mA and reveals that the NiO nanotube electrode has good cycle properties as an excellent electrode material for electrochemical capacitors.

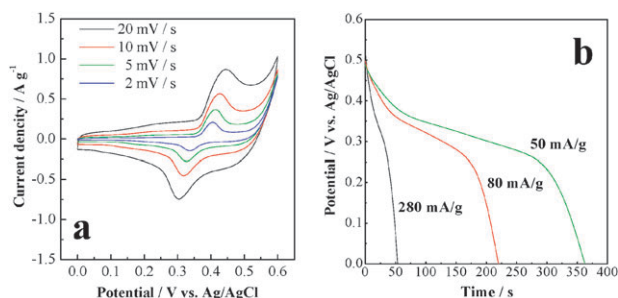
The magnetic properties of 1D nanomaterials are believed to be highly dependent on the structure, morphology, and geometry of the materials, such as the diameter and aspect ratio. Fig. 4 shows the field dependence of magnetization of NiO nanotubes measured by using quantum design MPMS SQUID XL-7. From Fig. 4, there exist small hysteresis loops at lower field at both temperatures, indicating the existence of a weak ferromagnetic component. This result suggests that the obtained NiO nanotubes are ferromagnetic and different from the bulk NiO, which is antiferromagnetic. The magnetic hysteresis loops show the coercive force ( $H_c$ ) values and the saturated magnetic ( $M_s$ ) moment at 1.8 K are 130.50 Oe and  $0.133 \text{ emu g}^{-1}$ , and 61.58 Oe and  $0.097 \text{ emu g}^{-1}$  at 300 K, respectively. This ferromagnetic behavior might be attributed to their 1D tube structures and very big aspect ratio.



**Fig. 2** (a)–(c) SEM images of NiO nanotubes obtained by calcining the Ni(dmg)<sub>2</sub> nanorods; (d) TEM image of NiO nanotubes (inset: HRTEM image and SAED pattern).

**Table 1** MICs (minimum inhibitory concentrations) ( $\mu\text{g mL}^{-1}$ ) of NiO nanotubes, NiO nanoflowers, and commercial NiO

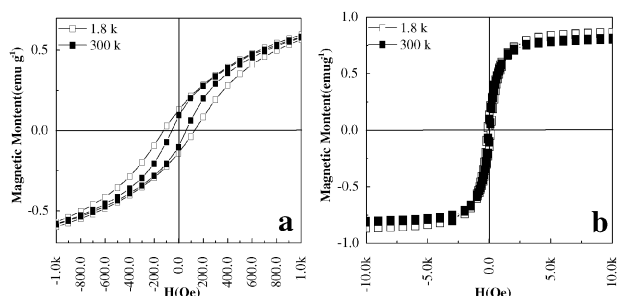
Samples	Minimum inhibitory concentration/ $\mu\text{g mL}^{-1}$				
	Gram positive			Gram negative	
	<i>B. subtilis</i>	<i>S. aureus</i>	<i>S. faecalis</i>	<i>P. aeruginosa</i>	<i>E. cloacae</i>
NiO nanotubes	6.25	6.25	25	6.25	25
NiO nanoflowers	> 50	50	> 50	50	50
Commercial NiO	> 50	> 50	> 50	> 50	> 50

**Fig. 3** (a) Cyclic voltammetric (CV) curves at different scan rates within a potential window of 0 to 0.6 V vs. Ag/AgCl; (b) discharge curves in the potential range from 0 to 0.5 V at different galvanostatic currents.

Meanwhile, these results suggest that there exist strong interactions among the nanoparticles of NiO nanotubes, resulting in a high saturation magnetization ( $M_s$ ).

This method not only provides us with NiO nanotubes with multi-functionalities, but is also an effective and facile route for other one-dimensional nanomaterials. Besides metal oxide, Ni/C nanocomposites can be obtained when using  $\text{N}_2$  as an inert atmosphere to calcine  $\text{Ni}(\text{dmg})_2$  nanorods with preservation of their morphology. The experimental details are described in the ESI†. Fig. S16 displays its XRD pattern, SEM and TEM images, suggesting that one-dimensional Ni/C nanostructure has also been successfully synthesized.

In summary, dimethylglyoxime, a common organic precipitant, has been employed for the synthesis of NiO nanotubes. The obtained NiO nanotubes show great antibacterial activities, electrochemical capacitance, and magnetic properties. The potential application of the synthesized NiO nanotubes in antibacterial application is promising, which may prevent bacteria colonization on prostheses, dental

**Fig. 4** Magnetization ( $M$ ) versus magnetic field ( $H$ ) of the NiO nanotubes taken at 1.8 K and 300 K: (a) from  $-1000$  Oe to  $1000$  Oe; (b)  $-10000$  Oe to  $10000$  Oe.

materials, stainless steel materials. We believe that research of the electrochemical capacitance and magnetic properties of NiO nanotubes are useful, which may be expected to lead to their use in a number of applications that involve magnetic drug delivery, MR imaging, nanoscale encapsulation, and so forth.

This work is supported by the National Natural Science Foundation of China (Grant No. 20671049, 20721002 and 50772047), the National Basic Research Program of China (Grant No. 2007CB925102), the Natural Science Foundation of Jiangsu Province (Grant No. BK2007129), and Program for New Century Excellent Talents in University.

## Notes and references

- S. W. Kim, M. Kim, W. Y. Lee and T. Hyeon, *J. Am. Chem. Soc.*, 2002, **124**, 7642.
- Y. G. Sun, B. Mayers and Y. N. Xia, *Adv. Mater.*, 2003, **15**, 7.
- Y. Yin, R. M. Rioux, X. K. Erdonmez, S. Hughes, G. A. Somorjai and A. P. Alivisatos, *Science*, 2004, **304**, 711.
- F. Caruso, R. A. Caruso and H. Möhwald, *Science*, 1998, **282**, 1111.
- N. Du, H. Zhang, B. D. Chen, X. Y. Ma and D. R. Yang, *Chem. Commun.*, 2008, 3028.
- M. Nath and C. N. R. Rao, *J. Am. Chem. Soc.*, 2001, **123**, 4841.
- X. Wang, X. M. Sun, D. P. Yu, B. S. Zou and Y. D. Li, *Adv. Mater.*, 2003, **15**, 1442.
- X. X. Li, F. Y. Cheng, B. Guo and J. Chen, *J. Phys. Chem. B*, 2005, **109**, 14017.
- S. H. Zhang, Z. X. Xie, Z. Y. Jiang, X. Xu, J. Xiang, R. B. Huang and L. S. Zheng, *Chem. Commun.*, 2004, 1106.
- X. F. Song and L. Gao, *J. Phys. Chem. C*, 2008, **112**, 15299.
- J. Park, E. Kang, S. U. Son, H. M. Park, M. K. Lee, J. Kim, K. W. Kim, H. J. Noh, J. H. Park, C. J. Bae, J. G. Park and T. Hyeon, *Adv. Mater.*, 2005, **17**, 429.
- X. Wang, L. Li, Y. G. Zhang, S. T. Wang, Z. D. Zhang, L. F. Fei and Y. T. Qian, *Cryst. Growth Des.*, 2006, **6**, 2163.
- J. X. Zhu, Z. Gui, Y. Y. Ding, Z. Z. Wang, Y. Hu and M. Q. Zou, *J. Phys. Chem. C*, 2007, **111**, 5622.
- G. Malandrino, L. M. S. Perdicaro, I. L. Fragalà, R. Lo Nigro, M. Losurdo and G. Bruno, *J. Phys. Chem. C*, 2007, **111**, 3211.
- C. S. Shi, G. Q. Wang, N. Q. Zhao, X. W. Du and J. J. Li, *Chem. Phys. Lett.*, 2008, **454**, 75.
- S. Manna, A. K. Deb, J. Jagannath and S. K. De, *J. Phys. Chem. C*, 2008, **112**, 10659.
- L. Tschugaeff, *Ber. Dtsch. Chem. Ges.*, 1905, **38**, 2520.
- K. Yamamoto, T. Kamata, Y. Yoshida, K. Yase, F. Mizukami and T. Ohta, *Adv. Mater.*, 1998, **10**, 1018.
- J. Meletiadis, J. F. Meis, J. W. Mouton, J. P. Donnelly and P. E. Verweij, *J. Clin. Microbiol.*, 2000, **38**, 2949.
- H. Pang, F. Gao and Q. Y. Lu, *Chem. Commun.*, 2009, 1076.
- T. Yuranova, A. G. Rincon, C. Pulgarin, D. Laub, N. Xantopoulos, H. J. Mathieu and J. Kiwi, *J. Photochem. Photobiol., A*, 2006, **181**, 363.
- W. Sugimoto, H. Iwata, Y. Yasunaga, Y. Murakami and Y. Takasu, *Angew. Chem., Int. Ed.*, 2003, **42**, 4092.